

## BCSJ Award Article

# External Quantum Efficiency and Electroluminescence Spectra of BIODÉ (Biomolecular Light-Emitting Diode) Fabricated from Horse-Heart Cytochrome *c*

Shingo Ikeda, Hiroyuki Tajima,\* Masaki Matsuda, Yoriko Ando, and Hidefumi Akiyama

The Institute for Solid State Physics, The University of Tokyo, Kashiwa 277-8581

Received March 9, 2005; E-mail: tajima@issp.u-tokyo.ac.jp

We fabricated organic light-emitting diodes (OLED) from horse-heart cytochrome *c*, and measured the electroluminescence (EL) spectra, current–voltage and EL intensity–voltage characteristics. The external quantum efficiency evaluated from those characteristics was  $6\text{--}8 \times 10^{-8}$  at an applied voltage of 13 V. The EL spectrum shows the Soret band around 400 nm, the Q band around 500 nm, and the 690 nm band. The three bands became obscure for a sample prepared in an acidic solution (pH = 1.68) and in a basic solution (pH = 10.01). Based on the energy diagram of the /ITO/cytochrome *c*/Al/ junction, we considered the difference in the EL spectrum from the photoluminescence or absorption spectrum.

The thin-film organic light-emitting diode (OLED) was fabricated by Vincett et al. for the first time.<sup>1</sup> This device is of interest not only for practical use, but also for basic research. By fabricating this device, we can measure the electro-luminescence (EL) spectra of insulating organic compounds, and can study their electrical and optical properties simultaneously. The EL spectra have not been much studied for organic compounds.

Recently, we succeeded to obtain the EL spectra of cytochrome *c* and myoglobin by using the OLED technique.<sup>2,3</sup> This is the first report on the fabrication of a biomolecular light-emitting diode (“BIODE”). In this paper, we report on the external quantum efficiency and the EL spectra of BIODÉ devices fabricated from cytochrome *c*. We discuss the characteristic feature of the EL spectrum of heme proteins.

Cytochrome *c* is a relatively low-molecular-weight protein that functions as an electron carrier in living systems. The crystal structures of cytochrome *c* obtained from several living systems were revealed by an X-ray diffraction technique. According to these studies, the structures are similar, at least around the iron-porphyrin, which is called heme *c* (Fig. 1).<sup>4,5</sup> The iron atom in the porphyrin ring is axially coordinated by histidine (His) and methionine (Met) groups, and exists in either oxidized Fe(III) or reduced Fe(II).<sup>4,5</sup>

### Experimental

Horse-heart cytochrome *c* was purchased from Wako Pure Chemical Industries. Thin films of cytochrome *c* (horse heart) were fabricated on an ITO electrode from an aqueous solution (0.9 wt % of cytochrome *c* in ultra-pure water) by a spin-coating technique. The thickness of the film was estimated to be  $\sim 500$

Å by the optical interference method. An Al electrode was formed on cytochrome-*c* film by the vacuum evaporation technique. The current–voltage characteristics were measured by using a volt meter (34420A Agilent) and a programmable electric source (7651 Yokogawa). The emission intensity was evaluated by using a Si photo-diode sensor and an electrometer (TR8652 Advantest). The EL spectra and emission images were measured by using a 15 cm monochromator and a nitrogen-cooled back-illumination-type CCD (Roper scientific).

### Results and Discussion

**Current–Voltage Characteristics, EL Intensity–Voltage Characteristics, and External Quantum Efficiency.** Current–voltage characteristics were measured by applying negative voltages to an Al electrode and positive voltages to an ITO

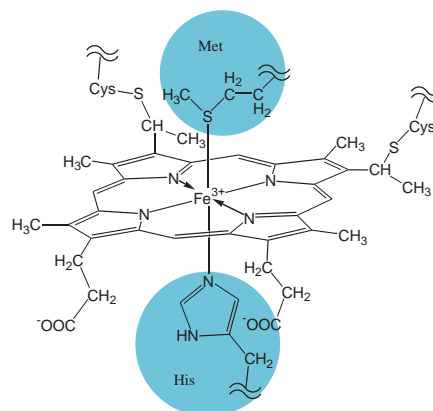


Fig. 1. Molecular structure of heme in oxidized cytochrome *c*.

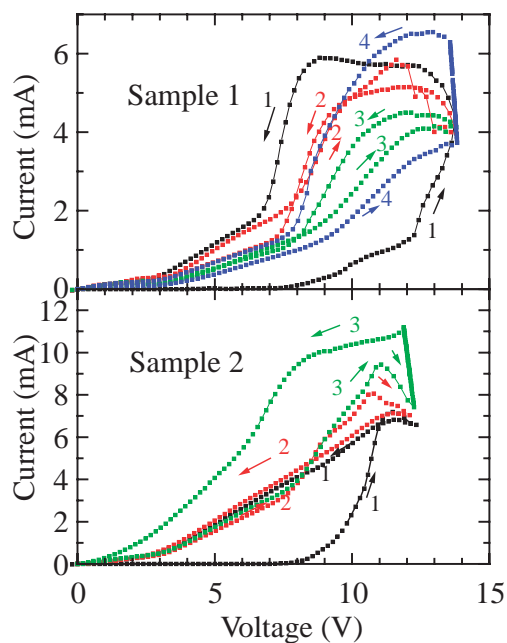


Fig. 2. Current–voltage characteristics of ITO/cytochrome *c*/Al junction.

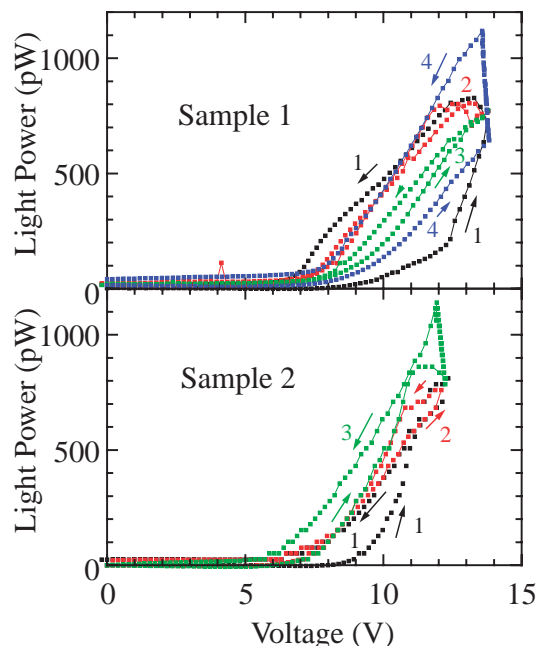


Fig. 3. EL intensity–voltage characteristics of ITO/cytochrome *c*/Al junction.

electrode. When the bias voltage was inversely applied, the current flow was negligible.<sup>2</sup> Figure 2 shows the  $I$ – $V$  characteristics for two samples. The bias voltages were increased from zero to  $\sim 13$  V, and then reduced to zero in one cycle. This voltage cycle was repeated several times for each sample. In the first increasing step of the voltage, there is a threshold around 8 V above which the current increases. This behavior was observed in all of the measured samples. As can be seen from the figure, however, other current–voltage characteristics were not reproducible, even for one sample.

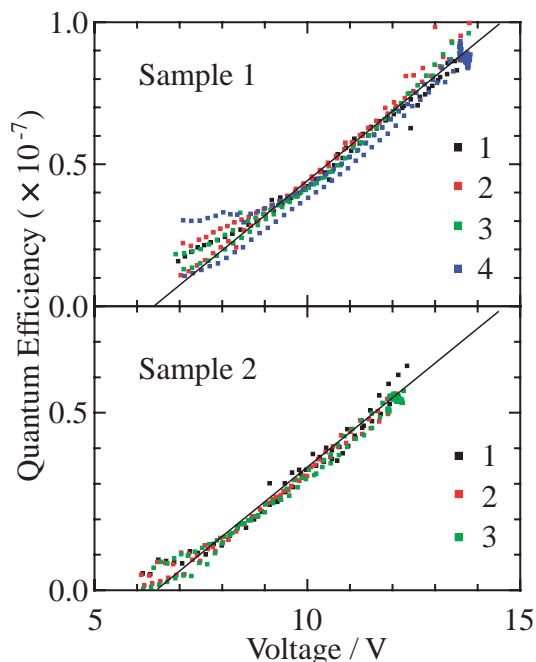


Fig. 4. Voltage dependence of the external quantum efficiency, derived from the current–voltage (Fig. 2) and EL intensity–voltage characteristics (Fig. 3).

Figure 3 shows the emission intensity versus the bias voltage measured simultaneously with the current shown in Fig. 2. Similar to Fig. 2, the emission intensity was also not reproducible, even for one sample. When we examine the two figures carefully, however, we find some similarity in both of them.

The external quantum efficiency of the OLED is defined as the probability that a single photon is emitted when a single electron pass across the junction. This quantity is proportional to the EL intensity and inversely proportional to the current. In order to evaluate the absolute value of the external quantum efficiency, the sensitivity of the photodiode sensor and the shape of the EL spectrum should be also taken into account. The shape of the EL spectrum did not exhibit any voltage dependence. We could thus evaluate the external quantum efficiency directly from the data shown in Figs. 2 and 3. Figure 4 shows the external quantum efficiency plotted as a function of the applied voltages. Interestingly, the external quantum efficiencies were reproducible for all the voltage cycles. Moreover, this quantity was consistent within 20% error in all the cytochrome-*c* devices measured. In view of the curves shown in Figs. 2 and 3, the consistency of the external quantum efficiency is surprising. This result suggests that the variance of the current–voltage and EL intensity–voltage characteristics are not due to degradation of the electrodes nor to the formation of the pinholes, but to the change of the current pathway.

In order to investigate this possibility, we simultaneously measured the current–voltage characteristics and the images of the ITO electrode on the light emission. Figure 5 shows the current–voltage characteristics and the images of the electrode. In this measurement, we repeated the voltage cycle three times.

Picture A is an image at  $V = 12$  V in the first increasing step of the voltage. This picture shows that light emission occurred

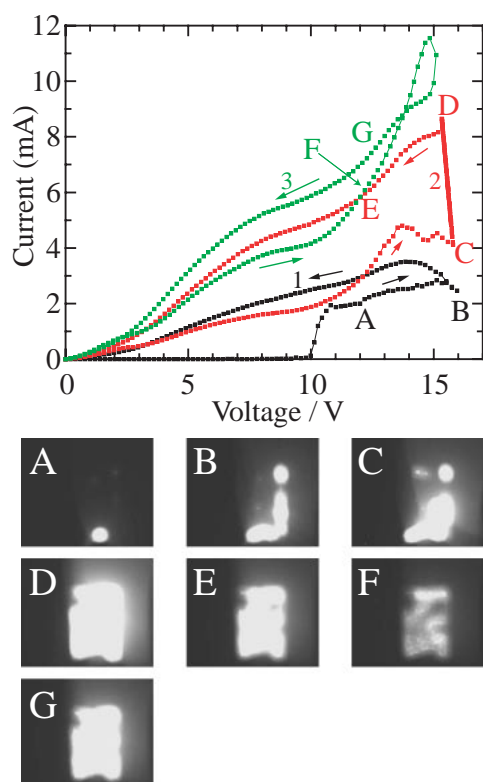


Fig. 5. The current–voltage characteristics and the images of the light-emitting areas in the electrode.

only in a part of the electrode in the first step. The subsequent pictures (B–D) show an increase of the emitting area during the voltage cycles. These pictures prove that the change of the current pathway occurs in this BIOD device. The last pictures (E–G) show that the area does not decrease, once it spreads over the entire region of the electrode. In this state, the emission intensity decreases, or increases, all over the electrode. This may suggest that the change of the current pathway is not a unique source of the non-reproducible behavior of the current–voltage and EL intensity–voltage characteristics.

#### Effect of the pH on the Electroluminescence Spectra.

The natural form of oxidized cytochrome *c* exists in the pH range of 2.5–9.<sup>5</sup> Outside of this range, structural changes of the protein occur. According to the literature, the absorption band at 690 nm is a sensitive probe into such structural changes.<sup>5</sup> This band strongly appears in the native form of cytochrome *c* around pH = 7 and becomes obscure with decreasing or increasing pH. In order to examine whether or not similar changes occur in the EL spectra, we prepared cytochrome-*c* films using buffer solutions at pH = 10.01 and at pH = 1.68. At pH = 1.68, cytochrome *c* is in the molten globule state, where the heme in cytochrome *c* is believed to be a mixture of high-spin and low-spin species and the three-dimensional structure of cytochrome *c* is partially lost.<sup>5</sup> At pH = 10.01, the cytochrome *c* is still in the low-spin state, but axial coordination of the heme is changed.<sup>5</sup>

Figure 6 shows the EL spectra of the cytochrome-*c* films prepared under different pH conditions. The three emission bands (~400 nm [Soret band]; ~500 nm [Q band]; 690 nm band) observed in a sample prepared in water became obscure

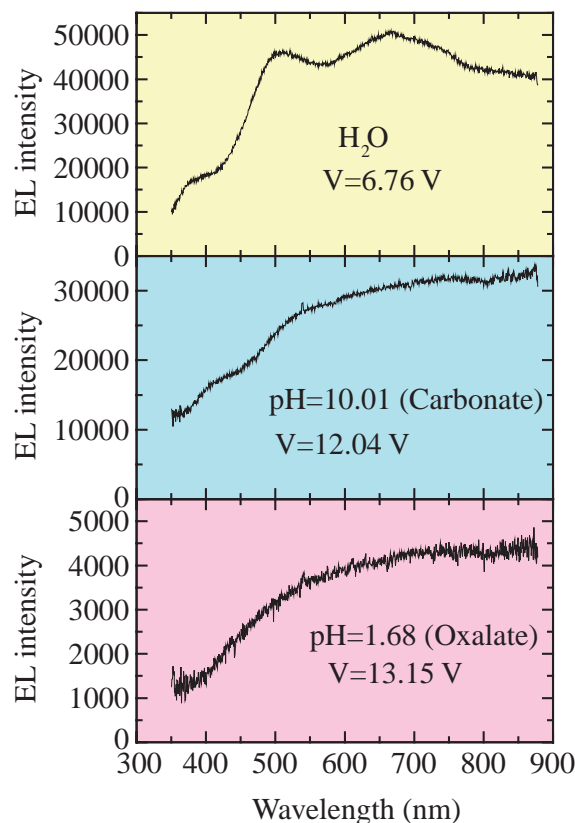


Fig. 6. The EL spectra of cytochrome-*c* films prepared from aqueous (top panel), basic (middle panel), and acidic (bottom panel) solutions, respectively.

in samples prepared under acidic and basic conditions. The 690 nm band became unclear in both spectra, while the Soret and Q bands were weakly observed in the spectrum at pH = 10.01. This is consistent with the changes of the 690 nm band in the absorption spectra. The emission intensity at pH = 1.68 is especially low. This is probably due to the lost of the three dimensional structure at this pH value. Generally, a cytochrome-*c* BIOD fabricated in acidic and basic conditions rapidly deteriorated under the applied voltages. Poor quality of the films formed under acidic and basic conditions may cause this rapid deterioration of the devices.

**Explanation of Electroluminescence Spectra Based on the Schematic Energy Diagram.** As shown in Fig. 6, the three broad emission bands (~400 nm [Soret band]; ~500 nm [Q band]; 690 nm band) appear in the EL spectra. The intensities of the three bands are comparable to each other in the EL spectra. According to photoluminescence (PL) studies by Champion et al.,<sup>6</sup> the oxidized cytochrome *c* does not show any fluorescence, and the reduced cytochrome *c* shows a very low yield of the Q-band fluorescence when excited into the Soret or Q band.<sup>7</sup> There is no report on an observation of the 690 nm band in the PL experiments. The absorption spectrum of cytochrome *c* exhibits the three bands.<sup>5,8</sup> However, the intensity of the 690 nm band in the absorption spectrum is much weaker than that of the Soret or Q bands. Since the intensities of the three bands in the EL spectra are comparable to each other, the spectral features of the EL spectra are different either from those of the absorption spectra or of the PL spectra. In

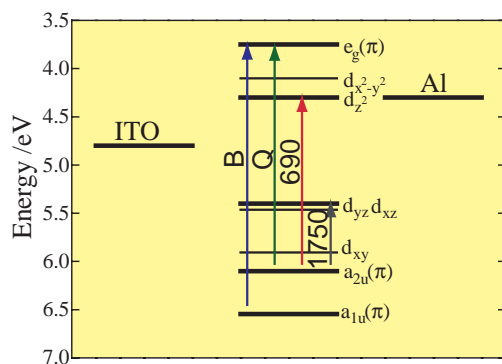


Fig. 7. Schematic energy diagram of /ITO/ferricytochrome *c*/Al/ junction. B: Soret band; Q: Q band; 690: 690 nm band; 1750: 1750 nm band (MCD). The energy levels of  $e_g(\pi)$ ,  $d_{z^2}$ ,  $d_{yz}$ ,  $a_{2u}(\pi)$ , and  $a_{1u}(\pi)$  are estimated on the basis of the work function given by UPS spectroscopy and assignment of optical transitions. (See the text.) The levels of  $d_{x^2-y^2}$ ,  $d_{xz}$ , and  $d_{xy}$  are not determined.

the following part of this article, we give a qualitative explanation of why the 690 nm band is enhanced in the EL spectrum.

Figure 7 shows a schematic energy diagram of the /ITO/ferricytochrome *c*/Al/ junction. The energy structure of heme and the assignments of the optical transitions in this diagram are essentially the same as those described by Fedurco.<sup>9</sup> The oxidized cytochrome *c* has a hole in the  $d_{yz}$  orbital, while the lower  $d_{xy}$  and  $d_{xz}$  orbitals are fully occupied. We determined the energy levels in this diagram by the following way: (1) We adopted the energy levels of the  $\pi$  orbitals ( $a_{2u}$ ,  $a_{1u}$ ) determined by the UPS method.<sup>10,11</sup> (2) The energy levels of  $e_g$ ,  $d_{z^2}$ , and  $d_{yz}$  are estimated from the orbital energies of the ( $a_{2u}$ ,  $a_{1u}$ )  $\pi$  bands and excitation energies of the three optical transitions ( $a_{2u} \rightarrow e_g$ ;  $a_{2u} \rightarrow d_{z^2}$ ;  $a_{2u} \rightarrow d_{yz}$ ). The configuration interaction is not taken into account, although it is important especially in the case of Soret- and Q-band excitations. (3) The orbital energies of  $d_{xy}$ ,  $d_{xz}$ , and  $d_{x^2-y^2}$  are not determined in this diagram.

This energy diagram shows that the Al cathode has a closer work function to the Fe  $d_{z^2}$  orbital than to the  $e_g(\pi)$  orbital. In such a case, electrons are expected to be more easily injected into the  $d_{z^2}$  orbital than to the  $e_g(\pi)$  orbital, when a voltage is applied. Thus, the emission intensity of the  $\pi$ - $d$  transition (690 nm band) is enhanced in the EL spectra. Contrary to the EL spectra, the PL and the absorption spectra directly reflect the optical transition probability. The  $e_g \rightarrow d_{z^2}$  transition is a forbidden transition in the  $D_{4h}$  symmetry. Thus, the electrons excited into the  $e_g(\pi)$  orbital (by the Soret- or Q-band excitation) hardly fall into the  $d_{z^2}$  orbital, although the  $D_{4h}$  symmetry is partially lost in cytochrome *c*. This explains why the 690 nm emission is absent in the PL spectra previously reported. The  $a_{2u} \rightarrow d_{z^2}$  transition is not a forbidden transition, even in the  $D_{4h}$  symmetry. However, the probability (consequently the absorbance) of the  $a_{2u} \rightarrow d_{z^2}$  transition (the 690 nm band) should be small, since the overlap between the two orbitals is small.

At the end of this section, we briefly discuss the B and Q bands in the EL and PL spectra. These bands do not, or hardly, appear in the PL spectra of heme proteins. However, they appear in the PL spectra when iron in the heme is replaced by

zinc.<sup>12</sup> This suggests that a vacancy in the Fe *d*-orbitals enhances the non-radiative energy-transfer process. In the EL spectra (Fig. 6), we have observed the B and Q bands in addition to the 690 nm band. Therefore, we assume that electrons are injected not only into the vacant *d*-orbitals, but also into the degenerate  $e_g(\pi)$  orbitals. In other words, we assume a multi-electron-excitation state in the EL-excitation process. Since the vacancy in the Fe *d*-orbitals is small in this state, the non-radiative transition for electrons injected into the  $e_g(\pi)$  orbital should be suppressed, and consequently the B and Q bands should appear in the EL spectra. These considerations seem to be consistent with the observations.

In conclusion, we have observed the light emission attributable to the Soret ( $\pi$ - $\pi^*$ ), Q ( $\pi$ - $\pi^*$ ), and 690 nm ( $d$ - $\pi^*$ ) bands in the cytochrome-*c* BIOD. The external quantum efficiency almost linearly increases for applied voltages above 6 V, and reaches to  $6\text{--}8 \times 10^{-8}$  at an applied voltage of 13 V. Based on the schematic energy diagram shown in Fig. 7, we successfully explained the difference in the EL spectrum from photoluminescence or absorption spectrum. EL spectroscopy is a promising technique to study complicated molecules, such as biomolecules. This technique enables one to inject carriers directly to molecules, and to detect an optical transition that is not easily detected by ordinary spectroscopic methods. Moreover, it provides electrical information as well as optical information.

This work was supported by a Grant-in-Aid for Scientific Research on Priority Areas of Molecular Conductors (No. 15073207) from the Ministry of Education, Culture, Sports, Science and Technology, Japan. The authors thank to Prof. Naoki Sato (Institute for Chemical Research, Kyoto University) for valuable discussion on the UPS spectroscopy of biomolecules.

## References

- 1 P. S. Vincett, W. A. Barlow, R. A. Hann, and G. G. Roberts, *Thin Solid Films*, **94**, 171 (1982).
- 2 H. Tajima, S. Ikeda, M. Matsuda, N. Hanasaki, J. Oh, and H. Akiyama, *Solid State Commun.*, **126**, 579 (2003).
- 3 H. Tajima, S. Ikeda, K. Shimatani, M. Matsuda, Y. Ando, J. Oh, and H. Akiyama, *Synth. Met.*, in press.
- 4 D. Voet and J. Voet, "Biochemistry," Wiley, New York (1995).
- 5 R. A. Scott and A. G. Mauk, "Cytochrome *c*: A Multidisciplinary Approach," University Science Books, California (1996).
- 6 P. M. Champion and G. J. Perreault, *J. Chem. Phys.*, **75**, 490 (1981).
- 7 According to Ref. 6, the authors mentioned the possibility of the Soret-band emission. However, this is not a definite conclusion.
- 8 W. A. Eaton and R. M. Hochstrasser, *J. Chem. Phys.*, **46**, 2533 (1967).
- 9 M. Fedurco, *Coord. Chem. Rev.*, **209**, 263 (2000).
- 10 K. Kimura, N. Sato, S. Hino, T. Yagi, and H. Inokuchi, *J. Am. Chem. Soc.*, **100**, 6564 (1978).
- 11 S. Kitagawa, I. Morishima, T. Yonezawa, and N. Sato, *Inorg. Chem.*, **18**, 1345 (1979).
- 12 H. Murakami and T. Kushida, *J. Lumin.*, **58**, 172 (1994).